Decadal scale variability of sea surface temperature in the Mediterranean Sea in relation to atmospheric variability

**Nikolaos Skliris · Sarantis Sofianos · Athanasios Gkanasos · Anneta Mantziafou ·
Vasilis Vervatis · Panagiotis Axaopoulos · Alex Lascaratos**

Abstract Twenty-four years of AVHRR-derived sea surface temperature (SST) data (1985–2008) and 35 years of NOCS (V.2) in situ-based SST data (1973–2008) were used to investigate the decadal scale variability of this parameter in the Mediterranean Sea in relation to local air–sea interaction and large-scale atmospheric variability. Satellite and in situ-derived data indicate a strong eastward increasing sea surface warming trend from the early 1990s onwards. The satellite-derived mean annual warming rate is about 0.037°C year^{-1} for the whole basin, about 0.026°C year^{-1} for the western sub-basin and about 0.042°C year^{-1} for the eastern sub-basin over 1985–2008. NOCS-derived data indicate similar variability but with lower warming trends for both sub-basins over the same period. The long-term Mediterranean SST spatiotemporal variability is mainly associated with horizontal heat advection variations and an increasing warming of the Atlantic inflow. Analysis of SST and net heat flux inter-annual variations indicates a negative correlation, with the long-term SST increase, driving a net air–sea heat flux decrease in the Mediterranean Sea through a large increase in the latent heat loss. Empirical orthogonal function (EOF) analysis of the monthly average anomaly satellite-derived time series showed that the first EOF mode is associated with a long-term warming trend throughout the whole Mediterranean surface and it is highly correlated with both the Eastern Atlantic (EA) pattern and the Atlantic Multidecadal Oscillation (AMO) index. On the other hand, SST basin-average yearly anomaly and NAO variations show low and not statistically significant correlations of opposite sign for the eastern (negative correlation) and western (positive correlation) sub-basins. However, there seems to be a link between NAO and SST decadal-scale variations that is particularly evidenced in the second EOF mode of SST anomalies. NOCS SST time series show a significant SST rise in the western basin from 1973 to the late 1980s following a large warming of the inflowing surface Atlantic waters and a long-term increase of the NAO index, whereas SST slowly increased in the eastern basin. In the early 1990s, there is an abrupt change from a very high positive to a low NAO phase which coincides with a large change in the SST spatiotemporal variability pattern. This pronounced variability shift is followed by an acceleration of the warming rate in the Mediterranean Sea and a change in the direction (from westward to eastward) of its spatial increasing tendency.

Keywords Mediterranean Sea · Sea surface temperature · AVHRR · Trends

1 Introduction

Due to its size and limited exchange at the Gibraltar Strait, Mediterranean Sea dynamics is mainly linked to the local climate and it is therefore particularly sensitive to climatic/anthropogenic perturbations. Variations in the climatic forcing cannot be compensated for by the Atlantic inflow but mainly by variations in the water mass characteristics of the basin (Bethoux and Gentili 1999). Several studies have demonstrated the rapid surface warming of the Mediterranean Sea during the last decades. Rixen et al. (2005), based on the

---

N. Skliris (✉) · S. Sofianos · A. Gkanasos · A. Mantziafou ·
V. Vervatis · P. Axaopoulos · A. Lascaratos
Ocean Physics and Modelling Group, Department of Environmental
Physics and Meteorology, University of Athens,
University Campus, PHYS-5,
15784 Athens, Greece
e-mail: nskliris@oc.phys.uoa.gr

MEDATLAS in situ measurements (MEDAR Group 2002), found an increase in the average temperature of the upper 150-m layer of the Mediterranean Sea of about 0.5°C in 1980–2000. Belkin (2009) estimated a much higher SST rise of 1.4°C from 1978 to 2003, at a rate of 0.056°C/year, which is one of the highest warming rates observed in the world's ocean over the considered period. Warming trends have been also observed both in the deep and intermediate layers of the Mediterranean Sea throughout the second half of the twentieth century (e.g. Bethoux and Gentili 1999; Rixen et al. 2005; Vargas-Yáñez et al. 2010). A few studies using satellite AVHRR-derived SST data also investigated the surface warming trends in the Mediterranean Sea during the last decades. Recently, Criado-Aldeanueva et al. (2008) reported a strong rise in the satellite SST of the whole Mediterranean in 1992–2005 at a rate of about 0.06°C/year, whilst Nykjaer (2009) found lower satellite SST increasing rates of about 0.03°C/year for the western and 0.05°C/year for the eastern Mediterranean sub-basins, respectively, over the 1985–2006 period.

SST variations are mainly controlled by variations in the air–sea heat flux as well as in the vertical mixing and the horizontal advection of heat. The inflow of North Atlantic surface waters at the Gibraltar strait represents an important source of heat for the basin, counterbalancing the net heat loss from the sea surface and from the Mediterranean outflow. The Mediterranean Sea is one of the first oceanic regions where the temperature increase was linked to greenhouse effects and global warming (Béthoux et al. 1990). Belkin (2009) argued that the observed rapid surface warming in the enclosed and semi-enclosed European Seas such as the Mediterranean, surrounded by major industrial/ population agglomerations, may have resulted from the observed large terrestrial warming directly affecting the adjacent coastal seas, whilst regions of freshwater influence seem to play a special role in modulating and exacerbating global warming effects on the regional scale. However, it is difficult to discriminate between the regional patterns of global climate change and the anomalies induced by natural low-frequency modes of large-scale atmospheric variability generally known to affect the Mediterranean climate such as that related to the North Atlantic Oscillation (NAO) and the East Atlantic (EA) pattern. On the other hand, it is also difficult to assess which part of the large-scale atmospheric variability is natural and which part is also induced by global climate change.

The NAO is associated with the strength of the meridional pressure gradient and the steering of storm tracks over the North Atlantic sector. The positive phase of the NAO is associated with stronger surface westerlies across the middle latitudes of the Atlantic onto Europe and with anomalous northerly flow across the Mediterranean (Hurrell et al. 2003). NAO is considered to be the key factor

influencing the precipitation field in the Mediterranean Sea, especially on decadal time scales (Jones et al. 1997; Mariotti and Dell'Aquila 2011). The large precipitation decrease in the Mediterranean Sea during the period 1960–1990 has been linked to a positive trend of the winter NAO index during the same period which induced a significant reduction of atmospheric moisture transport from the Atlantic (Hurrell 1995; Mariotti et al. 2002). Tsimplis and Josey (2001) suggested that changes in Mediterranean sea level are associated with the NAO variability. NAO also exerts a dominant influence on wintertime air temperature and SST of the Mediterranean Sea (Trigo et al. 2002; Hurrell and Deser 2009). Rixen et al. (2005), using the 50-year MEDATLAS climatology, provided evidence for consistent temperature changes in the Western Mediterranean and the North Atlantic, explained by similar heat fluxes anomalies which are strongly (positively) correlated to NAO. The East Atlantic Pattern is another prominent atmospheric low-frequency oscillation over the North Atlantic which plays an important role in modulating the European and Mediterranean climates (Barnston and Livezey 1987). Together with NAO, the EA pattern may explain much of the precipitation anomalies in the Mediterranean Basin (Quadrelli et al. 2001). The positive phase of the EA pattern is associated with above-average surface temperatures in Europe and the Mediterranean in almost all months and with below-average precipitation across southern Europe. Recently, Josey et al. (2011) demonstrated that the EA pattern has a much larger impact on the air–sea heat exchange in the Mediterranean Sea as compared to NAO. The Atlantic Multidecadal Oscillation (AMO) is another prominent climate pattern of the North Atlantic, which, in contrast with the other two low-frequency climate patterns which are mainly atmospheric variation modes (i.e. NAO and EA patterns), has its principal expression in the SST variability in the North Atlantic (Schlesinger 1994). Mariotti and Dell'Aquila (2011) found a close relationship between AMO and the Mediterranean SST at decadal timescales and suggested that AMO variability is transmitted to the Mediterranean Sea via atmospheric processes. Moreover, Marullo et al. (2011) found the presence of a significant oscillation of the Mediterranean SST with a period of about 70 years very close to that of the AMO.

Such teleconnections affecting the Mediterranean climate present a large temporal variability, with a strong seasonal cycle modulated on multi-decadal to centennial time scales (Lionello et al. 2006). Therefore, along with global warming effects on the regional scale, the North Atlantic climate variability is expected to play an important role in driving long-term trends in the Mediterranean Sea. In the present study, 24 years of AVHRR-derived SST daily data (1985–2008) and 35 years of NOCS in situ-derived

monthly data (1973–2008) are used to investigate the surface warming trend and its spatial distribution in the Mediterranean Sea. EOF and correlational analysis of the SST datasets is performed to assess the mechanisms controlling the SST decadal scale variability in the Mediterranean Sea in relation to variations in the heat input associated with the Atlantic water inflow, the air–sea heat exchange and the North Atlantic large-scale variability modes such as AMO, NAO and EA pattern.

2 Method

The construction of satellite-derived SST maps is based on a re-analysis of AVHRR Oceans Pathfinder (version 5.0) SST time series of the Mediterranean Sea (Marullo et al. 2007). A complete dataset of the 1985–2008 period consisting of declouded daily SST maps optimally interpolated on a 1/16° resolution-grid over the whole Mediterranean region was available from the Gruppo Oceanografia da Satellite (GOS) of the CNR (Consiglio Nazionale delle Ricerche)—ISAC (Istituto di Scienze dell'Atmosfera e del Clima). Marullo et al. (2007) validated the optimally interpolated Pathfinder SST dataset for the Mediterranean Sea using in situ data from 1985 to 2005, and they found a mean bias of less than 0.1 K with a root mean square error of about 0.5 K, whilst they showed that errors did not drift with time.

The inter-annual/decadal scale variability of the Mediterranean SST (1985–2008) is investigated herein by analysing the satellite-derived SST original time series as well as by performing an empirical orthogonal function (EOF) analysis of the anomaly SST time series. EOF analysis is considered to be a very efficient method to extract the most valuable information from large spatio-temporal datasets by reducing the original large information to a few dominant time-varying spatial patterns that explain most of the variance in the data. Recently, the EOF analysis of satellite-derived SST datasets has been proved to be an effective tool to investigate the spatiotemporal variability of various hydrodynamic features acting on a wide range of temporal and spatial scales, from coastal/regional circulation to global climatic patterns (e.g. Yoder et al. 2002; Venegas et al. 2008; Skliris et al. 2010). Herein, monthly averages of SST data are computed for the 1985–2008 period from the daily datasets to enable the dominant lower frequency patterns to be identified in the EOF analysis. Furthermore, in order to remove the very strong seasonal signal of the datasets that may mask the important long-term spatiotemporal variability signals, the stationary (harmonic) annual and semi-annual seasonal cycles are calculated and then subtracted from the monthly average SST at each grid point. This procedure removes only the stationary component of the

seasonality so that changes in phase and strength of seasonal cycles during the considered period contribute to non-seasonal anomalies (e.g. Venegas et al. 2008).

The singular value decomposition (SVD) method is used to perform the EOF analysis (Emery and Thomson 1998). The spatiotemporal data matrix $\mathbf{D}_{m \times n}$ is composed by m rows (number of pixels in each image) and n columns (number of images). Following the SVD method, the matrix D of rank r ($r = \min(n,m)$) can be uniquely decomposed in a matrix product of the form:

$$\mathbf{D} = \mathbf{USV^T}$$

where $\mathbf{U}_{m \times r}$ and $\mathbf{V}_{n \times r}$ are orthogonal matrices whose columns consist of the left and right singular vectors, respectively, and $\mathbf{S}_{r \times r}$ is a diagonal matrix containing the singular values. The left singular vectors represent the EOF spatial patterns, the right singular vectors represent the EOF amplitude time series, while the singular values are the square root of the EOF eigenvalues, which determine the variance explained by each EOF mode. The spatial amplitude of the EOF modes indicates the spatial distribution of the intensity of specific processes, while the temporal amplitude of the EOF modes indicates the time that a particular process is important. The combined spatiotemporal variability is obtained by multiplying the spatial and temporal amplitudes of each mode.

In order to investigate the relation of the obtained satellite-derived SST variability with in situ-derived SST variability, a longer in situ-based SST time series (1973–2008) but with much lower horizontal resolution is also constructed for the Mediterranean Sea derived from the National Oceanography Centre Southampton (NOCS) version 2.0 Surface Flux Dataset (Berry and Kent 2009). This is a global monthly mean gridded (1°×1 deg°) dataset of marine surface measurements and derived fluxes constructed using optimal interpolation. Input for the period 1973 to 2006 are ICOADS Release 2.4 ship data and the update from 2007 to 2008 uses ICOADS Release 2.5.

Moreover, in order to investigate the relation of the obtained SST variability with variations of local air–sea interactions, monthly time series of various atmospheric parameters/fluxes are also constructed for the Mediterranean Sea derived again from NOCS Version 2.0 Surface Flux Dataset (1973–2008). Monthly time series of air temperature (at 2 m above sea surface), shortwave radiation, longwave radiation, sensible heat, latent heat and net air–sea heat fluxes and their respective anomaly time series are constructed and compared through a correlational analysis with the anomaly SST time series.

Furthermore, in order to investigate the impact of low-frequency large-scale variability patterns on the Mediterranean SST, the winter (December–March) NAO index normalised

time series (Hurrell and Deser 2009), the EA pattern annual mean index time series (NOAA National Weather Service, Center for Climate Prediction, http://www.cpc.ncep.noaa.gov/data/teledoc/ea.shtml) and the AMO index (http://www.esrl.noaa.gov/psd/data/timeseries/AMO/) are also compared through a correlational analysis with the SST time series.

3 Results

3.1 SST linear trends

The analysis of the obtained SST monthly average dataset (1985–2008) is performed both at the Mediterranean basin scale and also at the sub-basin scale, i.e. the typical eastern and western sub-basins are considered (Fig. 1), in order to investigate if there is a different behaviour of the two sub-basins in terms of spatiotemporal variability patterns. Seasonal and annual mean spatially averaged SST time series are constructed and linear trends are calculated for all three basins. Basin-average yearly mean SSTs and linear trends are also computed in a $3°\times3°$ grid box in the Atlantic Ocean west of Gibraltar covering the Gulf of Cadiz in order to investigate the influence of inflowing surface Atlantic waters in the Mediterranean SSTs.

The total satellite-derived SST increase over the 1985–2008 period amounts to about 0.89, 0.62 and 1.01°C, for the whole basin, the western basin and the eastern basin, respectively (Fig. 2). The obtained annual mean warming rate is about 0.037°C year^{-1} for the whole basin, about 0.026°C year^{-1} for the western sub-basin and about 0.042°C year^{-1} for the eastern sub-basin. A similar warming trend with the western basin is also obtained in the Atlantic area near Gibraltar (0.025°C year^{-1}). Results for the satellite SST variations in the two sub-basins are in agreement with the study of Nykjaer (2009), based on the raw data of the same Pathfinder-derived SST dataset (i.e. as opposed to the optimally interpolated gridded version

of this dataset used in this study) over a slightly smaller period (1985–2006). The latter study shows a bit higher SST increasing rates for both the western (0.03°C year^{-1}) and eastern (0.05°C year^{-1}) sub-basins as compared to the present study over the same period. Criado-Aldeanueva et al. (2008) reported a satellite-derived SST increasing rate for the whole Mediterranean over the accelerated warming period 1992–2005 of about 0.06°C/year which is quite close to the warming rate of about 0.055°C/year obtained herein over the same period.

The NOCS SST basin-average yearly mean time series show an annual mean warming rate over 1973–2008 of about 0.025°C year^{-1} for the whole basin, of about 0.022°C year^{-1} for the western sub-basin and of about 0.026°C year^{-1} for the eastern sub-basin. NOCS SST time series demonstrates a quite similar decadal scale variability with the satellite-derived time series over their common period (1985–2008), indicating an acceleration of the warming rate from the mid-1990s onward (see Fig. 2). The correlation coefficient between yearly Mediterranean basin-average NOCS and satellite-derived SSTs over 1985–2008 is quite high ($r=0.89$, $p<0.01$), denoting the close relationship of the two estimated parameters. However, the satellite-derived dataset shows significantly higher warming rates for both sub-basins over the common 1985–2008 period (Table 1).

The spatial pattern of the satellite-derived SST linear trend over the 1985–2008 period (Fig. 3a) indicates a strong eastward increasing surface warming. Maximum SST warming trends are observed around the Cretan Arc and in the western part of the Levantine basin (>0.06°C year^{-1}) whilst minimal warming rates are observed in the Gibraltar Strait and the North Alboran basin (<0.01°C year^{-1}). Criado-Aldeanueva et al. (2008) reported a strong eastward increasing sea level rise in the Mediterranean sea over 1992–2005 mainly driven by the steric contribution of thermal origin which is consistent with the eastward increasing SST rise after 1992 obtained

Fig. 1 Basic geographic features of the Mediterranean Sea region. The *solid red line* defines the separation of the Mediterranean Sea in two sub-basins (east and west) where computations and statistics on the satellite-derived SST data are performed in the present study
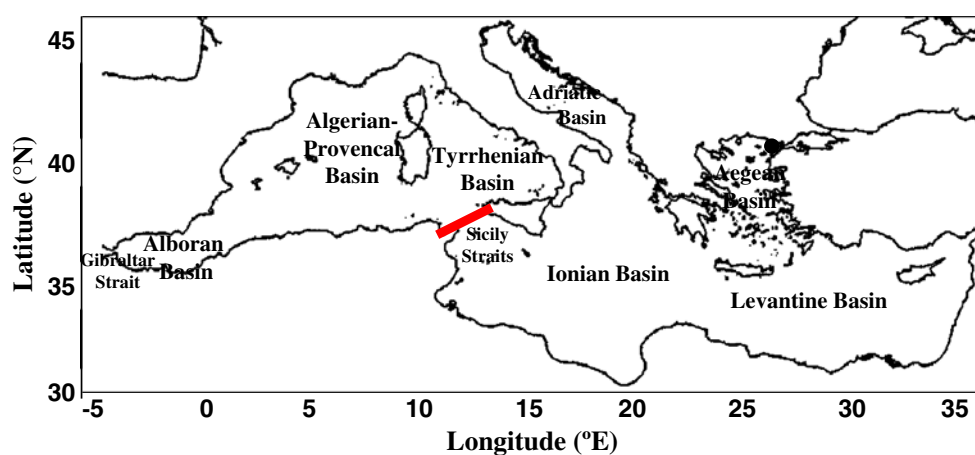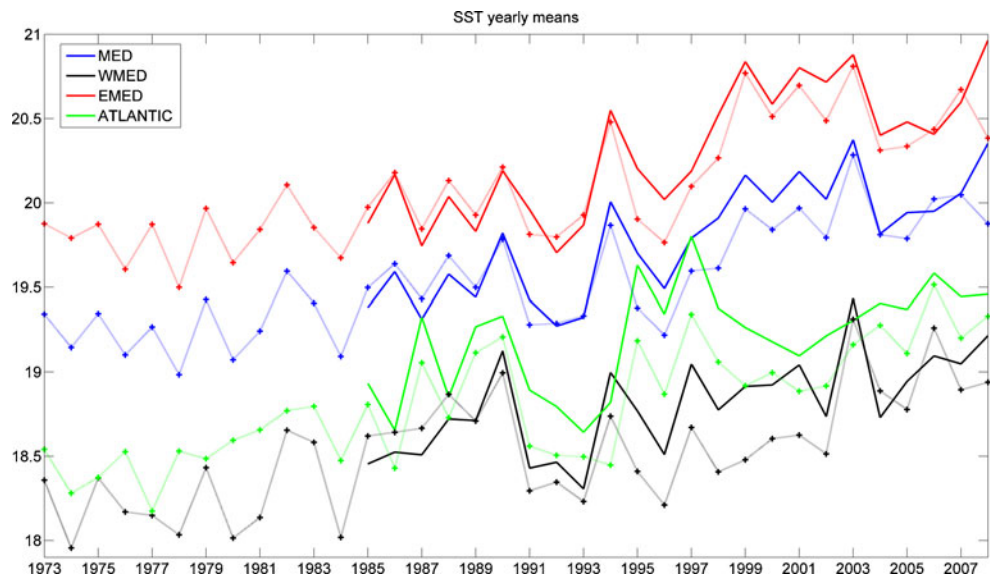
Fig. 2 Time series of basin-average yearly mean satellite-derived SST over 1985–2008 (*solid lines*) (**a**) and NOCS-derived SST (*dots and crosses*) over 1973–2008 (**b**) for the entire basin (*blue*), the western basin (*black*), the eastern basin (*red*) and the Atlantic area near Gibraltar (*green*)

in the present study. The above authors found maximum rates of sea level rise in the Levantine basin south of Crete closely around the same locations where the maximum SST warming trends are obtained herein.

A more thorough investigation of the time series shows that SST evolution has not a similar temporal behaviour in the two sub-basins and one may distinguish between two main periods of spatiotemporal variability. From 1973 until 1990, NOCS dataset indicates a small increasing SST trend in the eastern Mediterranean whereas SST warms more significantly in the western Mediterranean (see Table 1). During the same period, a relatively strong SST increasing trend is also obtained in the Atlantic area west of Gibraltar. Then, after a brief cooling throughout the whole area in the early 1990s, the warming rate considerably accelerates in the eastern basin followed by a lower warming rate in both the western basin and the Atlantic area west of Gibraltar. This pattern of eastward decreasing trend during the first period is also obtained by Lascaratos et al. (2003) who used the Comprehensive Atmosphere–Ocean Data Set data from 1945 to 1994 (da Silva et al. 1994) to study the long-term variability of SST in the three larger sub-basins of the Mediterranean Sea, namely, the Western, Ionian and Levantine basins. They also found a warming period from 1975 to 1990 with a strong eastward decreasing
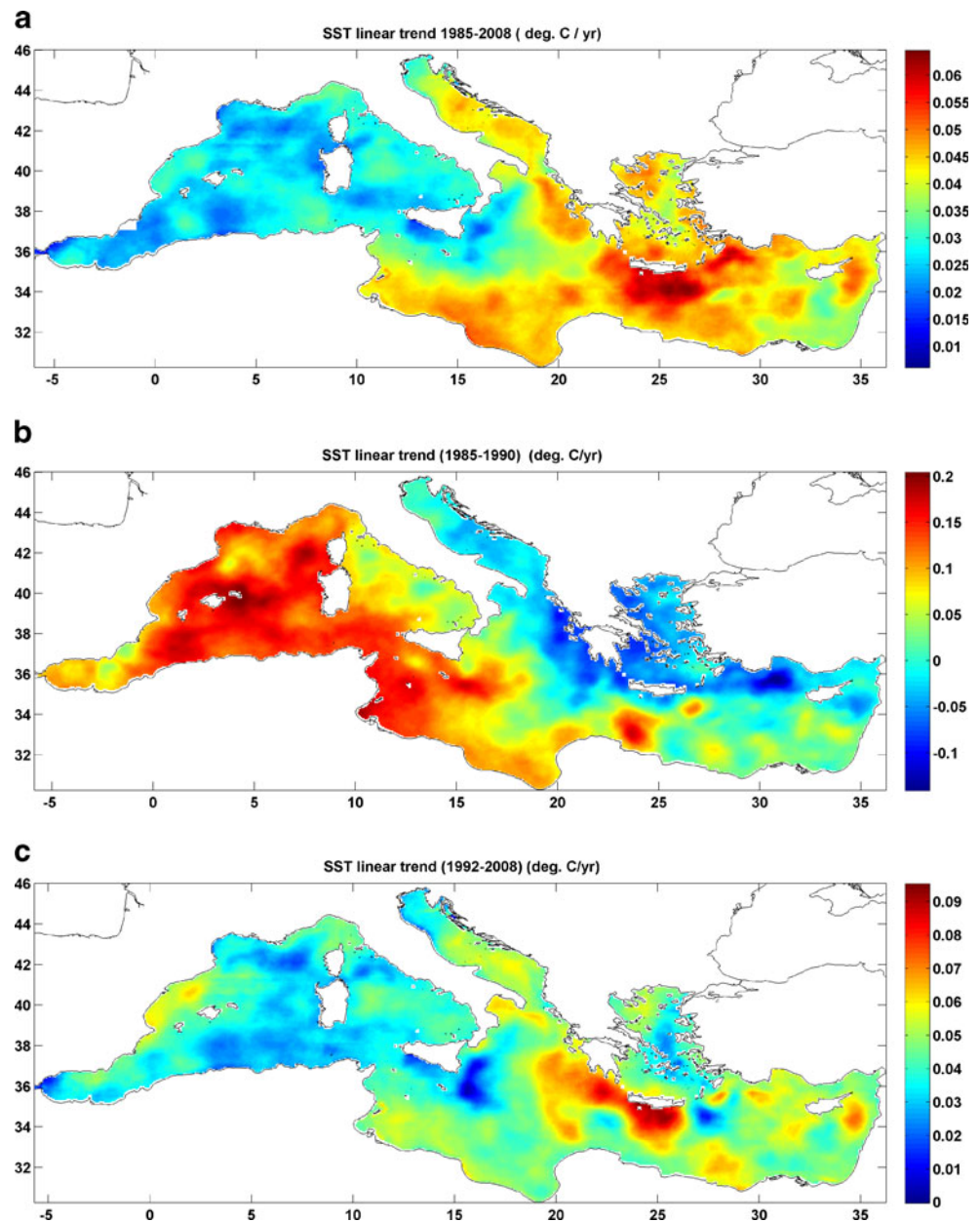
trend (i.e. the trend ranged from about 0.05°C year^{-1} in the western sub-basin to about 0.03°C year^{-1} in the Ionian basin and reaching almost zero in the Levantine basin). These authors suggested that the eastward decreasing trend was probably associated with an eastward advection of the warming western Mediterranean surface waters. The horizontal distribution of the satellite-derived SST temporal trend over the 1985–1990 period clearly shows an SST increase along the Modified Atlantic Water circulation path in the eastern basin, suggesting an eastward advection of the warming surface waters from the western basin (see Fig. 3b). The 1985–1990 period may be thus regarded as a transition period after which the horizontal increasing gradient in the SST temporal trend changed from the westward to the eastward direction (see Fig. 3c).

Satellite-derived seasonal mean time series show a marked seasonality in the SST linear trends (1985–2008) with much higher warming rates during spring/summer than in autumn/winter for both sub-basins (Table 2). In particular, large seasonal variability is observed in the temporal trend of the western basin, in which the warming rate is very high in spring (~0.054°C year^{-1}) whereas it is almost zero in autumn (~0.006°C year^{-1}). Results for the NOCS-derived SST seasonal mean time series indicate

Table 1 Linear trends of yearly mean basin-averaged NOCS SST and satellite-derived SST time series for various sub-basins and time intervals (°C/year). All linear trends are statistically significant at the 95% confidence interval

	Satellite (1985–2008)	NOCS (1985–2008)	NOCS (1973–1990)	NOCS (1990–2008)	NOCS (1973–2008)
MED	0.037	0.026	0.028	0.037	0.025
East MED	0.042	0.031	0.020	0.038	0.026
West MED	0.026	0.017	0.044	0.034	0.022
ATLANTIC	0.025	0.024	0.041	0.031	0.024

Fig. 3 Horizontal distribution of satellite-derived SST annual linear trends (°C/year) over **a** 1985–2008, **b** 1985–1990, **c** 1992–2008

similar interannual variability and seasonality patterns with the satellite-derived time series over the common 1985–2008 period but with considerably lower trend values (see Table 2). A marked difference between the two datasets is encountered in the western basin during summer when there is no significant trend in the NOCS dataset as opposed to the strong warming trend in the satellite dataset. Results from both datasets clearly show the signature of the heat wave that occurred during the summer of 2003 on the SSTs of the western Mediterranean Sea (Fig. 4a). The obtained mean summer 2003 SST value for the West Mediterranean Sea is almost 2°C higher than the long-term summer mean. The exceptional warming of the western Mediterranean sea surface over that period is
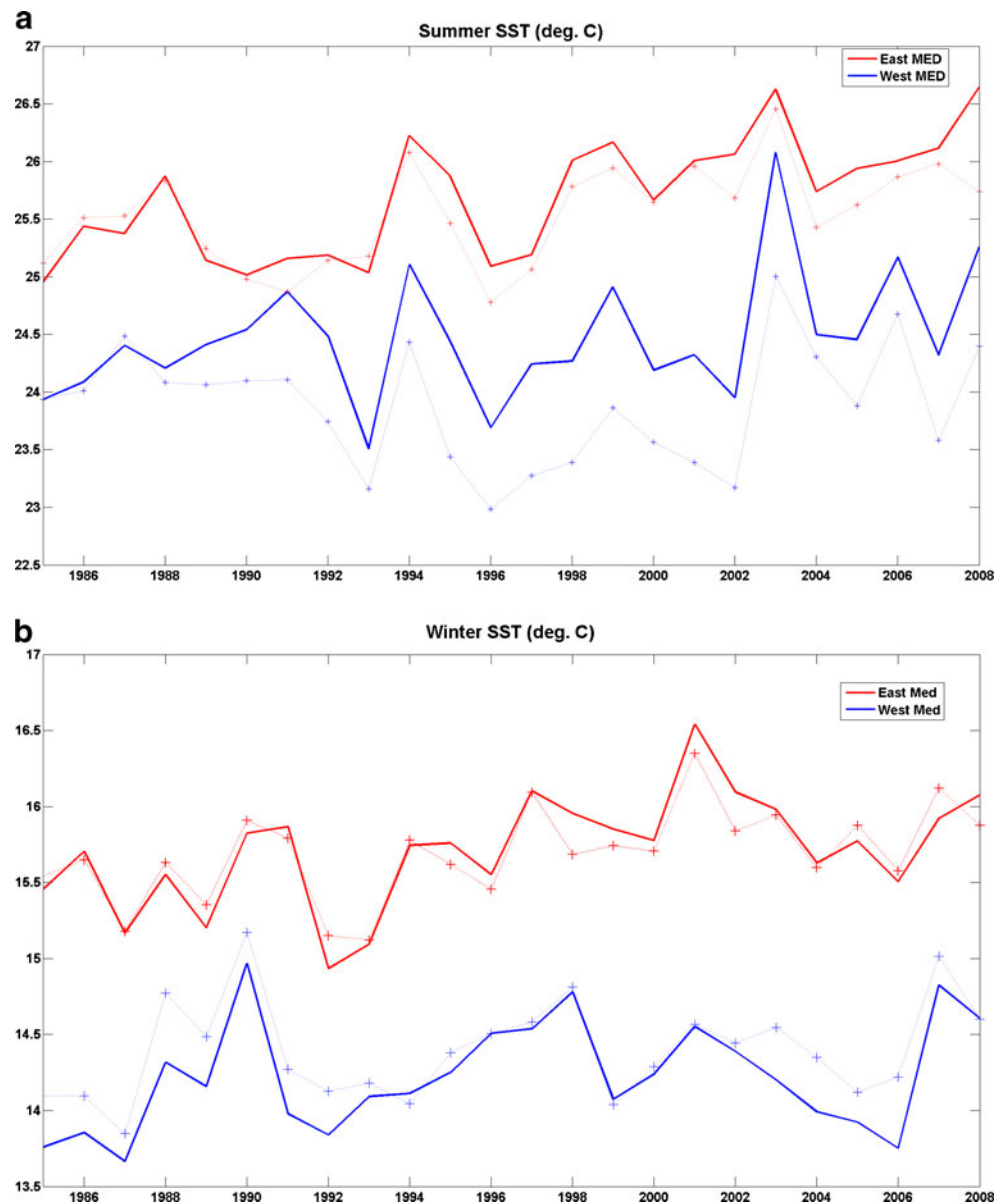
shown to induce an amplification of the heat wave over central Europe (Feudale and Shukla 2007). Summer SSTs

Table 2 Seasonal mean linear trends of yearly mean basin-averaged satellite-derived and NOCS-derived SST for the whole Mediterranean basin and for its two sub-basins over 1985–2008 (°C/year)

	MED Sat. NOCS	West MED Sat. NOCS	East MED Sat. NOCS
Spring	0.054 0.037	0.054 0.036	0.054 0.037
Summer	0.044 0.020	0.029 0.002[a]	0.051 0.030
Autumn	0.027 0.027	0.006[a] 0.014[a]	0.037 0.034
Winter	0.023 0.018	0.016 0.011[a]	0.026 0.022

[a] Trends that are not statistically significant at the 95% confidence interval

Fig. 4 Time series of basin-average seasonal mean satellite-derived SST (*solid lines*) and NOCS-derived SST (*dots and crosses*) over the 1985–2008 period for the western basin (*blue*) and the eastern basin (*red*) in **a** summer and **b** winter

in climate change scenarios are projected to increase well above the already high present values in the Mediterranean Sea (e.g. Christensen et al. 2007; Somot et al. 2008), and thus one may suggest that such warming episodes may be more frequent and extreme in the future. Mediterranean SST anomalies might even influence the climate of more distant regions. Rowell (2003) showed that anomalies of Mediterranean SSTs have a clear and significant impact on summer (wet season) rainfall over the Sahel. Years with warmer-than-average Mediterranean SSTs are often wetter over the Sahel due to the increase of moisture transport in the eastern part of the Sahara. The signature of the exceptionally cold winters of 1992 and 1993 is also clearly depicted on the winter SSTs of the Eastern Mediterranean (Fig. 4b). In particular, the obtained mean winter SST of the Eastern Mediterranean in 1992 is about 1 °C lower than the long-

term winter mean. Intense surface winter cooling during these 2 years is proven to be a key factor triggering the Eastern Mediterranean Transient in the early 1990s (Roether et al. 1996; Lascaratos et al. 1999; Josey 2003; Skliris et al 2007) associated with large dense water formation in the Aegean Sea which resulted in new, denser (much saltier but warmer) Aegean Sea waters replacing the old Eastern Mediterranean deep waters of Adriatic Sea origin.

3.2 SST EOF analysis

EOF analysis is applied herein to the high-resolution satellite-derived SST dataset to capture dominant space/time features of the non-seasonal variability of the Mediterranean Sea system. When the EOF analysis is applied to the original monthly average 1985–2008 time

series (not shown here), a large part of the variance is concentrated, as expected, on the strong seasonal cycle of SST. The first EOF of the SST original time series explained about 97% of the total variance, largely overwhelming the lesser modes. In this case, non-seasonal (intra-annual and inter-annual) signals are largely masked by the seasonal variability mode. In order to focus on the non-seasonal modes of variability, the stationary harmonic annual and semi-annual seasonal cycles are computed and subtracted from the original time series at each grid point before performing the EOF analysis. We quantified the percentage of variance represented by the stationary seasonal cycle and the non-seasonal signal by calculating the basin-averages of temporal variances at each grid point for both the original and the anomaly datasets. The original time series represents the total variability (seasonal cycle + non-seasonal signal), whereas the anomaly time series represents only the non-seasonal signal. As expected, the calculated non-seasonal variance accounts for only about 3% of the total variance.

EOF analysis of the SST anomaly dataset showing the spatial patterns and amplitude time series of each mode is depicted in Fig. 5. The first three SST EOF modes explain about 79% of the total non-seasonal variance of the data with the first mode alone explaining about 53%. The spatial pattern of the first mode (Fig. 5a) shows positive values throughout the domain, indicating an in-phase oscillation of the whole basin around the steady-state mean. The highest SST variability is observed in the central part of the basin with maximum amplitudes in the northern Adriatic Sea and the Tyrrhenian Sea, whereas minimum variability is observed in the Alboran Sea and in the eastern part of the Aegean Sea. The amplitude time series of the first mode (Fig. 5b) exhibits an alternation of positive and negative peaks throughout the year on timescales of a few months. The filtered amplitude time series of this mode indicates strong inter-annual modulations of the seasonal cycle's strength and a long-term positive trend following the general warming trend of the Mediterranean Sea. The largest positive peak of inter-annual variability is encountered in summer 2003, which is the warmest summer during the record, and the largest negative peak in winter 1992, which is the coldest winter during the record.

The second SST EOF mode accounts for about 21% of the total non-seasonal variance. Its spatial pattern (Fig. 5c) is a dipole showing opposite variation between the eastern and western sub-basins. In the eastern Mediterranean, maximum variability is obtained in the Levantine basin and the Aegean Sea whereas in the western Mediterranean maximum variability of opposite sign is observed offshore the Gulf of Lions. The EOF amplitude time series (Fig 5d) shows important both high-frequency (1–2 months) and interannual/decadal scale variability. The filtered time series
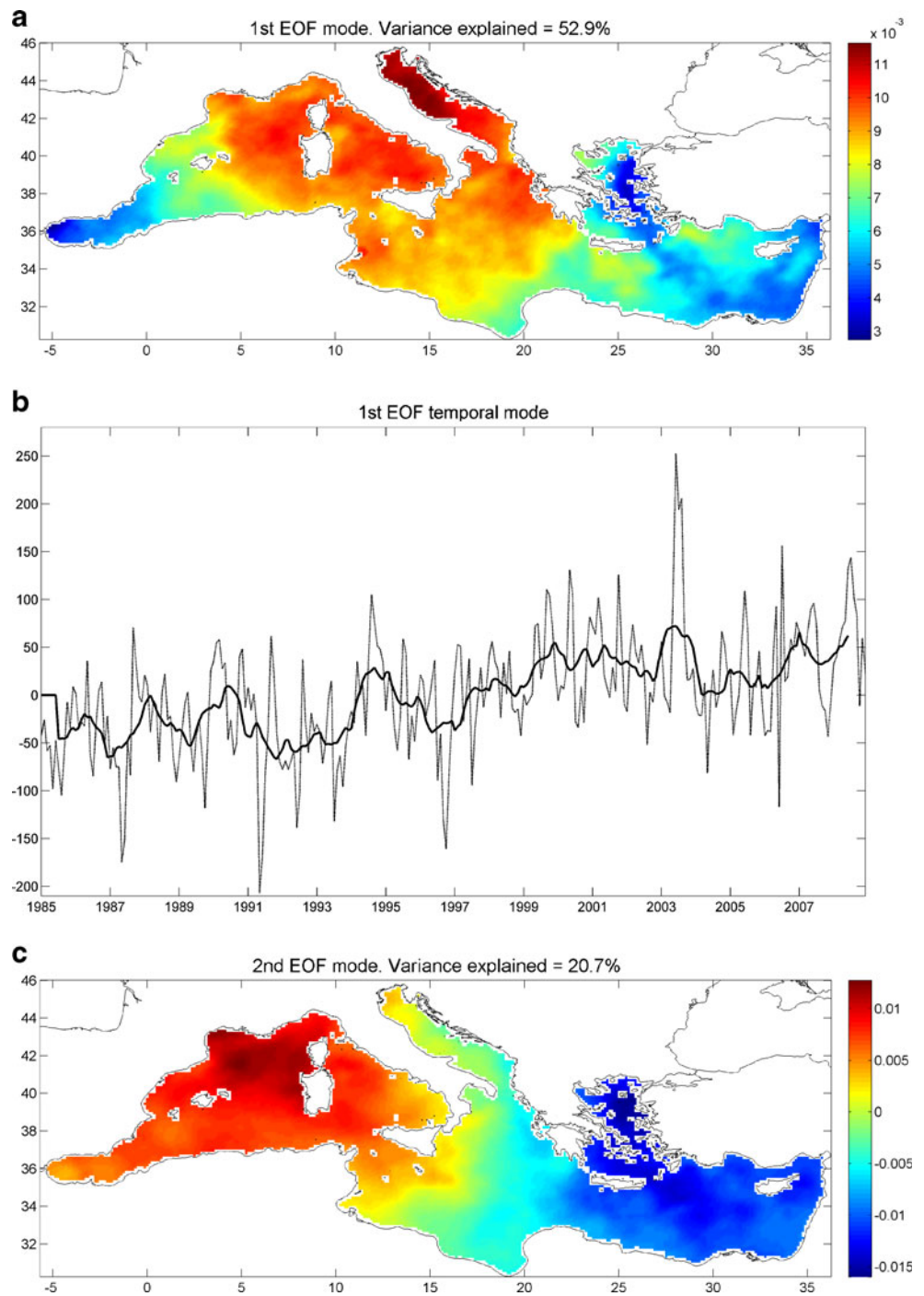
shows a clear trend from a mean positive to a mean negative variation period, indicating that the spatial variation pattern is reversed in the two sub-basins in the mid-1990s. Therefore, the second EOF mode superimposed on the first EOF mode (i.e. associated with a general warming trend throughout the basin) may largely explain the observed higher warming rate of the eastern basin as compared to the western basin during the second half of the record.

The third SST EOF mode accounts for about 5% of the total non-seasonal variance. The spatial distribution of this mode (Fig. 5e) shows an out-of-phase oscillation with opposite variation peaks between the central part of the basin (Tyrrhenian, Adriatic and Ionian basins) and the westernmost and easternmost parts of the basin. Maximum variability is observed in the Alboran Sea and the western part of the Algerian–Provencal basin. The filtered EOF amplitude time series (Fig. 5f) shows a rapid shift in the early 1990s with a strong 2-year negative variation period, whereas the rest of the record is characterised by low interannual variability with no particular trends. This abrupt variability shift in the third EOF mode coincides with the strong basin-average SST decrease in the Mediterranean during the early 1990s which is particularly pronounced in the western part of the basin.

3.3 SST vs. local air–sea interaction variability

The air-temperature-over-land anomalies in the Mediterranean region during the last five centuries indicate an unprecedented strong warming from the mid-1970s onwards, featuring the hottest summer decade 1994–2003 in the entire record (1500–2003) (Luterbacher et al. 2004; Xoplaki et al. 2006). Mediterranean SSTs obtained herein also show an exceptionally high warming during the 1994–2003 period, reaching about 1°C/decade, which is one of the highest warming rates recorded in the global ocean. The obtained yearly anomaly time series of both satellite-derived and NOCS in situ-derived SSTs and NOCS air temperature at 2 m above sea surface (T_{air}) are, as expected, highly correlated (satellite SST – NOCS T_{air} (1985–2008): $r=0.86$, $p<0.01$, NOCS SST – NOCS T_{air} (1973–2008): $r=0.93$, $p<0.01$). Analysis results for the NOCS-derived 1973–2008 air–sea heat flux components time series show that the largest part of net heat flux (Q_{net}) variability in the Mediterranean Sea is explained by the variability of the latent heat flux (Table 3). Radiative fluxes (i.e. short-wave and long-wave radiation) have much smaller variability (not shown) while sensible heat flux is one order of magnitude lower than latent heat flux, and thus all these components have a much smaller contribution to net heat flux anomalies. The net air–sea heat flux is highly anti-correlated (i.e. negatively correlated) with SST. Results clearly show a long-term decrease of the net heat

Fig. 5 EOF decomposition of the satellite-derived SST dataset (1985–2008): **a** first EOF spatial amplitude, **b** first EOF temporal mode, **c** second EOF spatial amplitude, **d** second EOF temporal mode, **e** third EOF spatial amplitude, **f** third EOF temporal mode. The variance explained by each EOF is also depicted. The unfiltered time series (dashed light lines) represents both intra-annual and interannual variability. The 13-month running mean (solid lines) highlights interannual variability
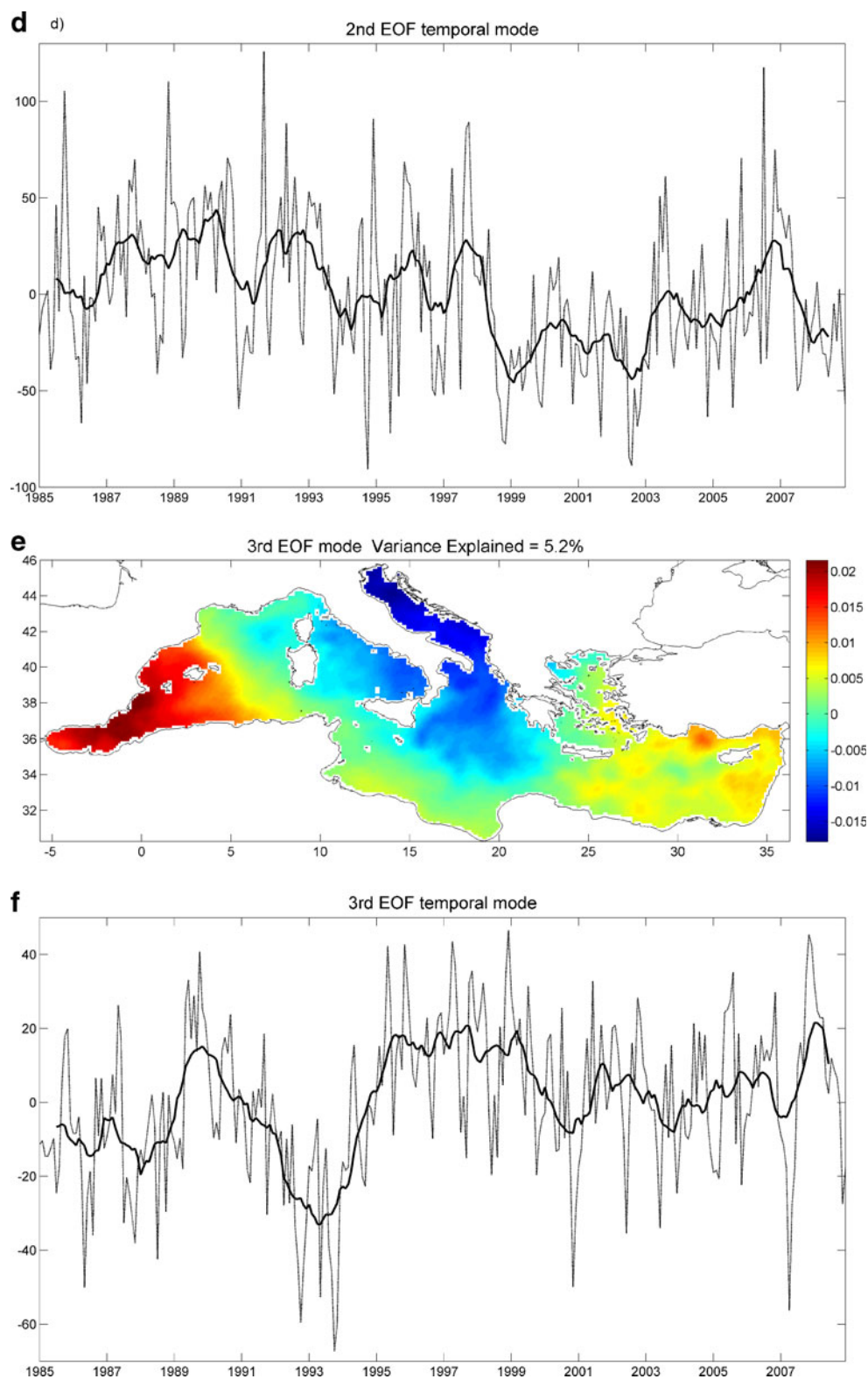

flux following the Mediterranean Sea surface warming trend over the 1973–2008 period (Fig. 6). Net heat flux variations very closely follow latent heat flux variations in both sub-basins, the latter being highly correlated with both the SST and SST minus T_{air} variations (Fig. 7; Table 4). These results suggest that the SST mainly drives the long-term air–sea heat flux variability in the Mediterranean Sea over the considered period through latent heat flux variations. Mariotti (2010) found an evaporation increase in the Mediterranean Sea from the mid-1970s onwards with higher increasing rates during

the 1990s mainly attributed to changes in the surface humidity gradient driven by the SST increase. This is in accordance with the SST-driven long-term latent heat loss increase obtained herein over the same period. Moreover, Romanou et al. (2010), based on satellite-derived data during 1988–2005, also found a large increase in the evaporation rate over the Mediterranean Sea which, in turn, was also associated with the SST increase.

One may distinguish between different co-variability periods of SST and Q_{net} in the two sub-basins over 1973–2008.

Fig. 5 (continued)

From 1973 to the mid-1980s, there is a long-term gradual decrease of air–sea heat flux while at the same time SST is increasing in both sub-basins (see Fig. 7), indicating that SST drives the air–sea heat flux. During the second half of the 1980s, there is an acceleration of the warming trend in the western basin associated with a large Q_{net} increase, suggesting that the atmospheric conditions now probably play a significant role in controlling the air–sea fluxes and the SST variations in the western basin. After a brief cooling period in the early 1990s with both SST and Q_{net} decreasing in both

Table 3 Correlation coefficients between yearly mean basin-averaged net heat flux (Q_{net}) and SST, latent heat flux, sensible heat flux, net shortwave radiation and net longwave radiation derived by the NOCS dataset (1973–2008) for the whole Mediterranean basin and for the western and eastern sub-basins, respectively

Q_{net}

	Med	W. Med	E. Med
SST	−0.66	−0.51	−0.72
Latent heat flux	0.96	0.97	0.95
Sensible heat flux	0.78	0.79	0.75
Shortwave radiation	0.30[a]	0.24[a]	0.35
Longwave radiation	−0.28[a]	0.16[a]	−0.44

[a] Correlations that are not statistically significant at the 95% confidence interval

sub-basins, the surface warming is accelerated throughout the whole Mediterranean. However, Q_{net} variations show a different behaviour in the two sub-basins. Whilst Q_{net} remains at high levels in the western basin, it gradually decreases in the eastern basin. The Q_{net} decrease in the eastern basin throughout the 1990s and 2000s is associated with an SST accelerated increase, suggesting again that the SST controls the net heat flux mainly through an increase of latent heat loss from the ocean. Importantly, there is a drastic abrupt decrease of the net heat flux in the western basin during the 2000s (particularly evidenced at the exceptionally warm year of 2003) that is clearly driven by the increase of latent and sensible heat loss, which in turn is associated with the large increase of SST with respect to T_{air} (see Fig. 7).

3.4 SST vs. large scale atmospheric variability patterns

The decadal-scale natural variability expressed by various low-frequency large-scale atmospheric modes is superim-posed to the long-term trends induced by global climate change effects on the regional scale of the Mediterranean Sea. A correlational analysis is performed herein to investigate the co-variability of the two major North Atlantic teleconnection patterns, namely, the NAO and EA patterns, and the SST variations in the Mediterranean Sea. Correlational analysis between SST and other teleconnection patterns known to have an impact on the Mediterranean climate such as the East Atlantic/West Russia pattern (e.g. Josey et al. 2011) showed low and not statistically significant correlations at inter-annual/decadal timescales.

The winter NAO index is generally defined as the difference between the normalised mean winter (December–March) sea level pressure anomalies at Lisbon, Portugal, and Stykkisholmur, Iceland (Hurrell 1995). Positive (negative) NAO index is often associated with warmer (cooler) conditions over the northwestern part of the Mediterranean Sea and cooler (warmer) conditions over the southeastern part (Trigo et al. 2002). The winter NAO index long-term variations indicate a large positive trend from the early 1970s until the early 1990s and then a negative trend until the mid-2000s (Hurrell and Deser 2009). The EA pattern is structurally similar to NAO but its north–south dipole of anomaly centres is displaced southeastward to the approxi-mate nodal lines of NAO (Barnston and Livezey 1987), containing a stronger sub-tropical link. The positive phase of the EA pattern is associated with above-average surface temperatures in Europe and the Mediterranean basin in almost all months. The EA pattern exhibits very strong multi-decadal variability, with the negative phase prevailing during much of 1950–1976 and the positive phase occurring during much of 1977–2004 (NOAA National Weather Service, Center for Climate Prediction, http://www.cpc.ncep.noaa.gov/data/teledoc/ea.shtml).

Both satellite-derived and in situ-derived basin-average SST yearly anomalies are highly (positively) correlated with

Fig. 6 NOCS-derived Mediterranean basin-average yearly mean anomaly time series of net air–sea heat flux (W/m²) (black), b) latent heat flux (W/m²) (red), and c) SST (°C) (blue) over the 1973–2008 period
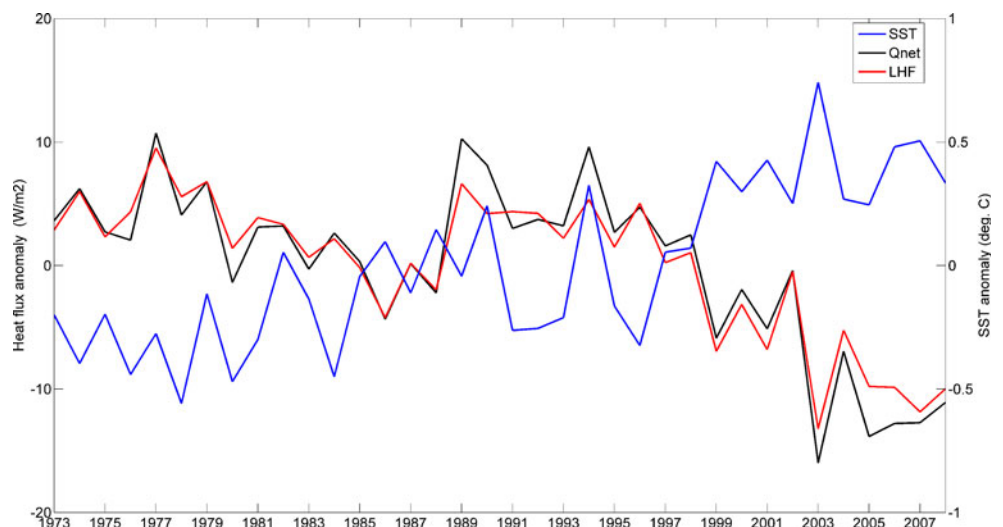
Fig. 7 NOCS-derived basin-average yearly mean anomaly time series of **a** net air–sea heat flux (W/m^2), **b** latent heat flux (W/m^2), **c** sensible heat flux (W/m^2), **d** SST and **e** SST minus T_{air} (°C) over the 1973–2008 period for the western (blue) and eastern (red) sub-basins
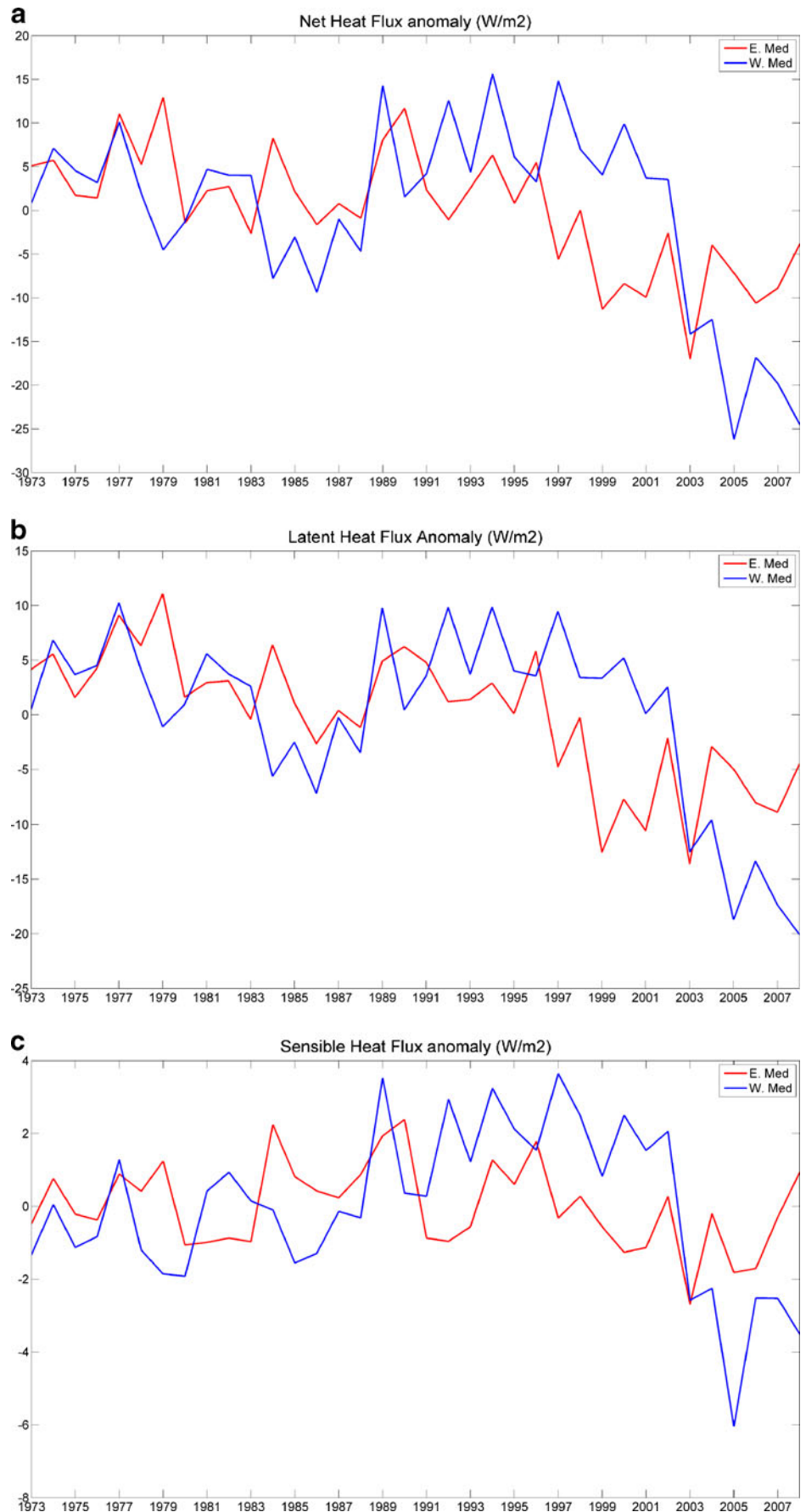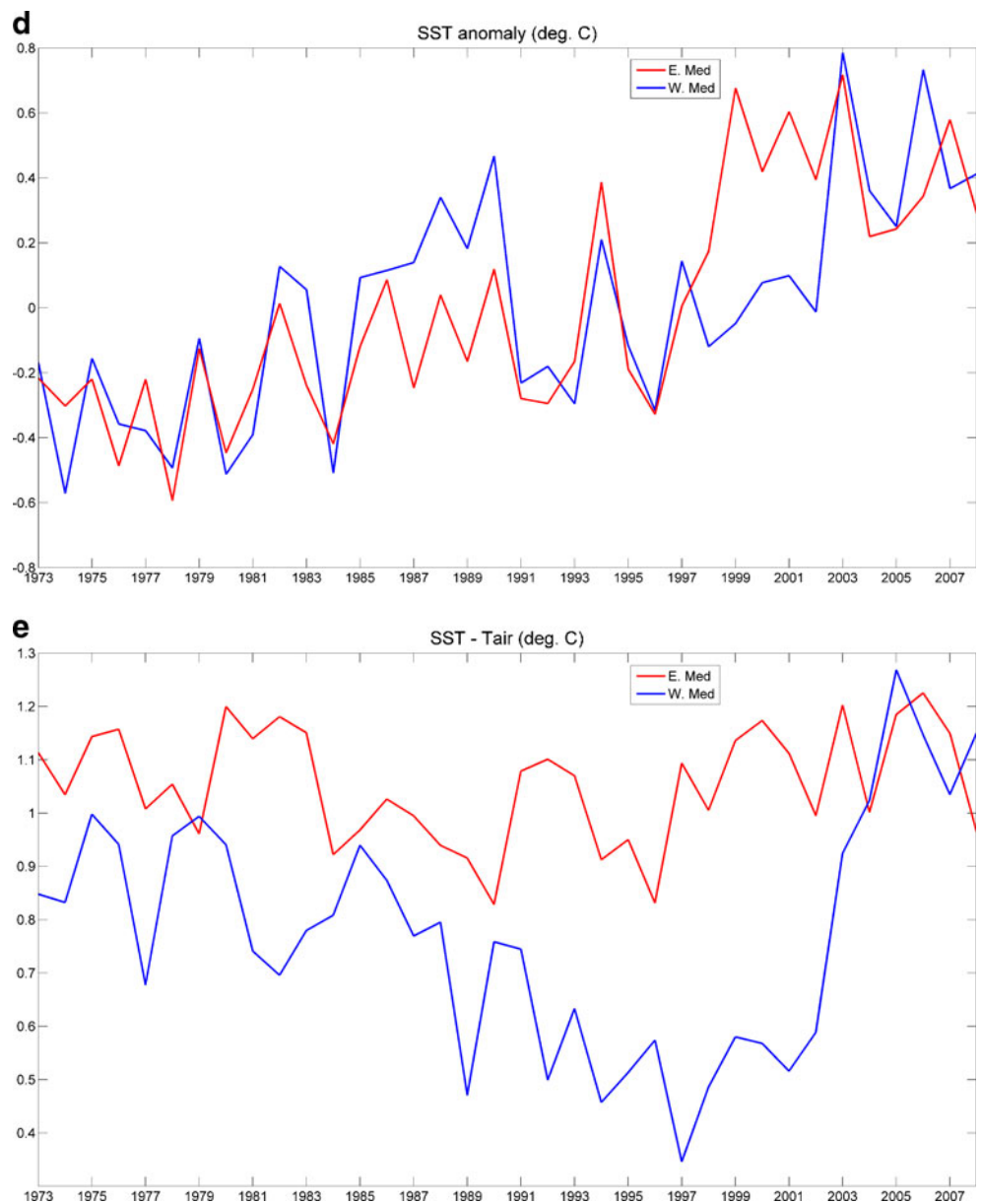
Fig. 7 (continued)

EA pattern yearly-mean index time series in both the eastern and western sub-basins (Table 5). Furthermore, the first EOF mode of SST yearly anomalies which shows an in-phase

Table 4 Correlation coefficients between yearly mean basin-averaged latent heat flux and SST/SST-T_{air} derived by the NOCS dataset (1973–2008) for the whole Mediterranean basin, and for the western and eastern sub-basins, respectively. All correlations are statistically significant at the 95% confidence interval

Latent heat flux

	Med	W. Med	E. Med
SST	−0.78	−0.58	−0.81
SST-T_{air}	−0.52	−0.76	−0.51

oscillation of the whole basin and is associated with a long-term warming trend throughout the Mediterranean Basin is highly (positively) correlated with EA pattern index yearly time series ($r=0.62$, $p<0.01$) (Fig. 8a). The other two EOF modes show much lower and no significant correlations with the EA pattern index. Josey et al. (2011) reported a major effect of the EA pattern on the net heat budget of the Mediterranean Sea with the positive phase of the EA pattern giving rise to reduced heat loss across the whole basin.

The obtained basin-average SST anomaly and NAO variations show low and not statistically significant correlations of opposite sign for the eastern (negative correlation) and western (positive correlation) sub-basins. This result is also consistent with the findings of Josey et al. (2011) who reported a small impact of NAO on the net heat budget of

Table 5 Correlation coefficients between yearly mean basin-averaged NOCS SST (1973–2008) and satellite-derived SST (1985–2008) and EA pattern/AMO/NAO indexes for the whole Mediterranean and for the western and eastern sub-basins, respectively
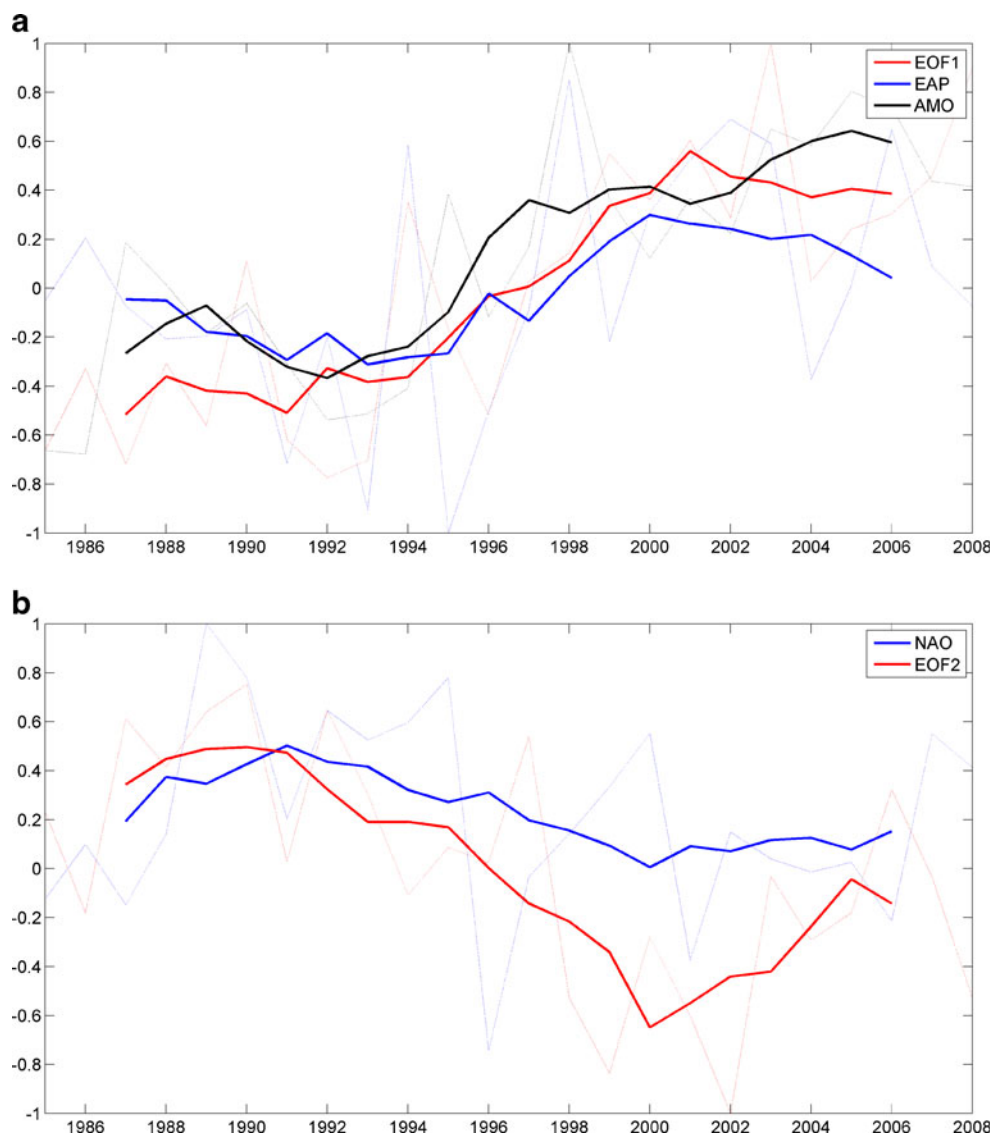
	Med SST		W. Med SST		E. Med SST	
	NOCS	Satellite	NOCS	Satellite	NOCS	Satellite
EA	0.67	0.56	0.58	0.52	0.66	0.55
AMO	0.68	0.65	0.67	0.62	0.59	0.61
NAO	−0.05[a]	−0.10[a]	0.14[a]	0.15[a]	−0.15[a]	−0.23[a]

[a] Correlations that are not statistically significant at the 95% confidence interval

both Mediterranean sub-basins as compared with the EA pattern. The above authors also showed the existence of an east–west dipole structure for the winter heat flux anomaly associated with NAO comparable to the one obtained herein for the SST anomaly. The yearly mean SST anomaly EOF amplitude time series of all three modes also show relatively low and not statistically significant correlations with the NAO index over the 1985–2008 period. However, results indicate a relationship between decadal-scale variations of the NAO index and the second EOF temporal mode (Fig. 8b), with the latter reflecting the different behaviour of the two Mediterranean sub-basins in terms of SST

Fig. 8 Normalised time series of **a** EA pattern index (*blue*), AMO index (*black*) and first EOF temporal mode of SST yearly anomalies (*red*) and **b** winter NAO index (*blue*) and second EOF temporal mode of SST yearly anomalies over the 1985–2008 period. The 5-year running means (*thick solid lines*) highlight decadal variability

spatiotemporal variability. There is a shift in the early 1990s from a very high to a low NAO phase that is closely followed by the change in direction of the SST spatial increasing tendency (i.e. from the westward to the eastward direction). Analysis of 5-year running means of second EOF temporal mode and winter NAO index time series (1985–2008) showed a large correlation coefficient ($r\sim0.8$) but still not statistically significant at the conventional 95% confidence interval due to the few independent data in the filtered time series (i.e. $p\sim0.1$). Figure 9 shows the horizontal distribution of correlation coefficients and corresponding p values for statistical significance between SST yearly anomaly and the winter NAO index time series at each grid point. Results indicate statistically significant and relatively high negative correlations ($r>0.5$, $p<0.05$) between yearly SST anomalies and NAO within the Tyrrhenian, Adriatic, Ionian and southern Levantine basins, whereas in the westernmost part of the domain low positive and not statistically significant correlations were obtained.
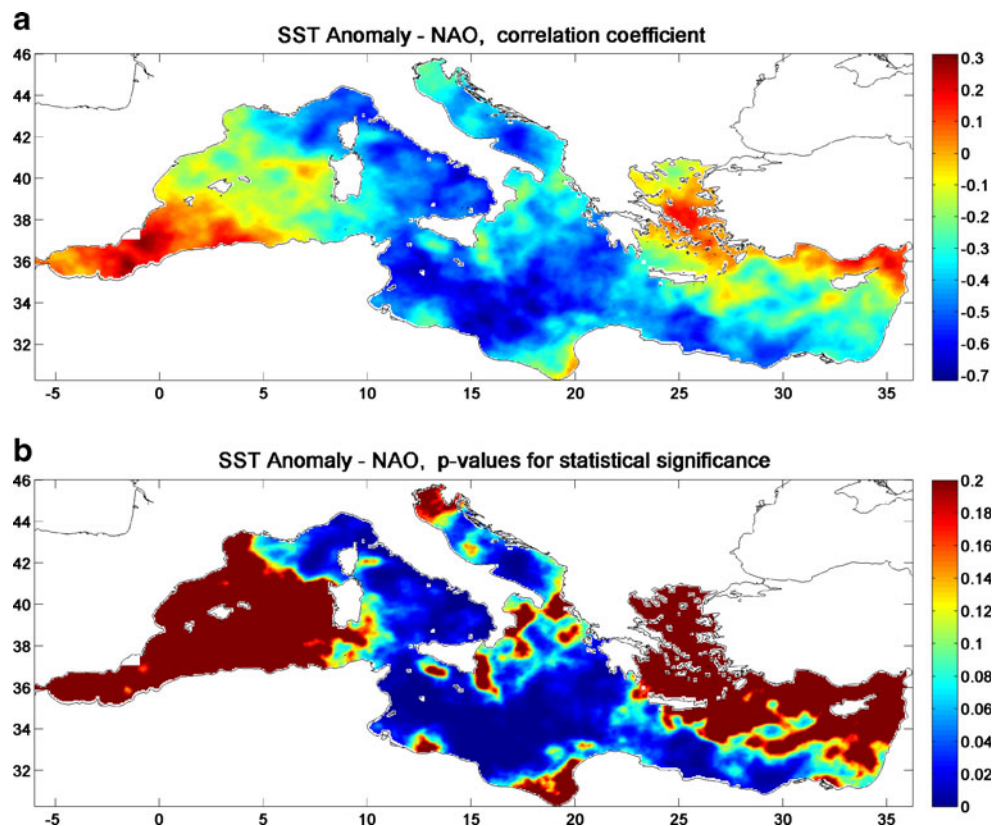
4 Discussion

The basin-scale increasing warming of the Mediterranean Sea surface that is highlighted in the first EOF mode of SST anomalies is closely linked with the EA pattern index increase during the same period and seems to follow the global warming trend which is accelerated after the early 1990s. SST yearly anomalies derived from both datasets are also positively correlated with the yearly mean AMO index (see Table 3). AMO variations show a long-term increase from a negative to a positive phase over 1973–2008. As for the EA pattern, a relatively high correlation coefficient is found between AMO and the first EOF mode of SST anomalies ($r=0.66$, $p<0.01$). Results are consistent with the study of Mariotti and Dell'Aquila (2011) who found a high correlation between AMO and the Mediterranean SST throughout the year over the period 1870–2009. These results indicate a close relationship between SSTs in the North Atlantic and the Mediterranean Sea. Vargas-Yáñez et al. (2010) showed that the long-term temperature variability in the upper 200-m layer of the western Mediterranean highly correlates with the heat absorbed by the upper North Atlantic Ocean.

SST variability in the two sub-basins is controlled by the net air–sea heat flux, as well as by local ocean processes such as horizontal advection and vertical mixing of heat. One may distinguish between different periods of SST spatiotemporal variability over 1973–2008 in relation to atmospheric variability and horizontal advection patterns. From 1973 to the mid-1980s, there is a gradual decrease of net air–sea heat flux in both sub-basins while at the same time SST is increasing but with a higher warming trend in the western basin than in the eastern basin. This could be

Fig. 9 Horizontal distribution of correlation coefficients (**a**) and corresponding p values for statistical significance (**b**) between time series of winter NAO and satellite-derived SST yearly anomalies at each grid point

explained by the advection of warmer Atlantic surface waters in the western Mediterranean as shown by the large SST increasing trend in the Atlantic area west of Gibraltar over the same period. It is interesting to note that the correlation between AMO and basin-average NOCS SST (1973–2008) is maximum in the Atlantic area west of Gibraltar and decreases eastwards (i.e. Atlantic: $r \sim 0.80$, $p < 0.01$; WMED: $r \sim 0.67$, $p < 0.01$; EMED: $r \sim 0.59$, $p < 0.01$). During the second half of the 1980s, there is an acceleration of the warming in the western basin associated with a large Q_{net} increase, suggesting that the atmospheric conditions now probably play a significant role in controlling the air–sea fluxes and the SST variations in the western basin. A brief surface cooling period occurred during the early 1990s that is more pronounced in the western basin, also associated with a more prolonged cooling in the Atlantic area west of Gibraltar. After the early 1990s, whilst surface warming is accelerated again throughout the whole Mediterranean, SST and Q_{net} variations show a different behaviour in the two sub-basins. The SST warming rate becomes larger in the eastern than in the western sub-basin whilst Q_{net} remains at high levels in the western basin and it gradually decreases in the eastern basin. Q_{net} decrease in the eastern basin seems again to be mainly driven by the increasing SST and the associated large latent heat loss. Therefore, local ocean processes such as horizontal advection of heat from the western basin and/or vertical mixing probably control the accelerated surface warming in the eastern basin. The Q_{net} increase in the western basin is associated with a moderate SST increase, suggesting that the atmospheric conditions probably modulate again the air–sea fluxes and along with the increasing warming trend in the inflowing surface Atlantic waters control the SST in the western basin. Although a low correlation is obtained between NAO and SSTs on interannual timescales, there seems to be a link between the two parameters on decadal timescales. An enhanced spatiotemporal variability shift is observed in the Mediterranean SST in the early 1990s that may partly be explained by the NAO index variations. NAO gradually increased throughout the 1970s and 1980s to reach a positive maximum value at the late 1980s and then rapidly decreased to negative or low positive values. As mentioned before, the high positive NAO phase is associated with warmer conditions over the western sub-basin and cooler conditions over the eastern, sub-basin while the contrary occurs during negative NAO phases. Over most of the 1973–2008 period, NAO index and Q_{net} (as well as NAO index and SST) are poorly correlated in both sub-basins as the large SST increase drives the air–sea heat flux decrease (i.e. through a latent/sensible heat loss increase). However, our results show that NAO index and Q_{net} yearly variations are highly (positively) correlated in the western basin over 1985–1995 ($r \sim 0.7$, $p < 0.05$) when atmospheric conditions seem to

control the net air–sea heat flux and the SST variations. In particular, the large SST increase in the western basin during the late 1980s seems to closely follow both NAO index and Q_{net} increase. In the early 1990s, a large atmospheric variability shift occurred as evidenced by the abrupt decrease of both Q_{net} and NAO index. This NAO-related atmospheric variability shift probably contributed to the change in the SST spatiotemporal variability pattern which is particularly depicted in the second EOF mode of SST anomalies and it is associated with the change in the direction of the SST spatial increasing tendency in the Mediterranean Sea (i.e. from the westward to the eastward direction).

Rixen et al. (2005), based on the MEDATLAS in situ measurements (MEDAR Group 2002), investigated the basin-average pentadal/decadal temperature variations for the upper 150 m layer as well as for the intermediate (150–600) and bottom (600–bottom) layers for the eastern and western Mediterranean basins from 1950 until 2000. The above authors showed a significant warming in the upper 150 m from the mid-1980s until 2000, except from a brief cooling period in the early 1990s, in both sub-basins in agreement with SST variations obtained herein. Significant temperature increases are also obtained after the mid-1980s for the bottom layer of both sub-basins, suggesting that the surface warming signal was rapidly propagated in the bottom layers via the deep water formation sites of both sub-basins. On the other hand, the authors showed a small decreasing temperature trend in the western basin and a marked cooling in the eastern basin upper 150 m layers from the 1970s until the mid-1980s as opposed to the SST increasing trends obtained for both sub-basins in the present study. This period is also characterised by a strong cooling of the intermediate layers throughout the Mediterranean (Rixen et al. 2005), which probably resulted in cooling of the overlying upper layers through mixing, but did not significantly affected the SSTs.

The long-term surface warming, and particularly the increase of winter SSTs, is expected to have an impact on the future thermohaline circulation of the Mediterranean Sea. A significant increase of winter SSTs may diminish dense water formation rates in the various deep/intermediate water formation sites of the basin and thus may slow down the thermohaline circulation. However, on the other hand, the evaporation increase which is driven by the SST rise combined with a precipitation decrease as observed during the last few decades (Mariotti 2010; Mariotti and Dell'Aquila 2011; Romanou et al. 2010) may enhance dense water formation by increasing surface salinity in the Mediterranean basin. Observations indicate that there is a discernible trend of increased salinity and warmer temperature in key Mediterranean water masses over the last 50 years and this "Mediterranean signal" of change is also clearly depicted in the North Atlantic intermediate waters

(Bindoff et al. 2007). Moreover, twenty-first century climate change scenario projections for the Mediterranean basin predict a further larger surface warming and drying of the basin (e.g. Somot et al. 2008). Rixen et al. (2005) suggested that the western Mediterranean deep water temperature being highly correlated with both the North Atlantic air–sea heat fluxes and the NAO index can be used as a proxy for climate change studies. Changes in the temperature/salinity of the Mediterranean outflowing water through the Gibraltar strait may influence the general circulation in the North Atlantic which is a major site of deep water formation controlling the global thermohaline circulation.

This study reveals the necessity to conduct more research that would dissociate interdecadal/multidecadal natural variability signals from global signals related with the present heat absorption of the oceans in the context of global warming in order to predict more accurately future climate changes in the regional scale as well as to assess the impact of regional climate changes on the global climate system. This is even more relevant in the case of a complex marine system such as the Mediterranean Sea where there is a superimposition of different low-frequency atmospheric signals and intense local ocean variability signals related to strong advection/mixing and intermediate/deep water formation.

5 Conclusions

The analysis of both the AVHRR and in situ-derived SST data indicates a strong warming of the Mediterranean Sea surface that is accelerated after the early 1990s. The satellite-derived dataset shows larger warming trends than the NOCS dataset for both sub-basins over the same period. EOF analysis of the satellite-derived SST anomaly time series shows that the basin-scale long-term warming that is highlighted in the first EOF mode is highly correlated with the EA pattern and the AMO index. The long-term Mediterranean SST spatiotemporal variability is mainly attributed to anomalous horizontal advection of heat and the warming of the Atlantic inflow rather than to local air–sea heat flux variations. Results show that the western Mediterranean SST evolution closely follows that of the Atlantic area west of Gibraltar, suggesting that the warming of the western basin could be at least partially induced by a warmer Atlantic inflow. Results indicate that the increasing SST drives a long-term net air–sea heat flux decrease in the Mediterranean Sea over the considered period through increasing latent heat loss from the ocean. On the other hand, the basin-scale long-term warming is superimposed to a decadal variability signal clearly depicted in the second EOF mode which seems to be associated with the inter-

decadal NAO variability. The latter EOF mode reflects a different behaviour of the two Mediterranean sub-basins in terms of spatiotemporal variability patterns. During 1973–1990, there is a significant SST rise in the western basin following a large warming of the inflowing surface Atlantic waters and a long-term increase of the NAO index, whereas SST slowly increased in the eastern basin. After a brief cooling period in the early 1990s for both sub-basins and a change from a high positive to a low NAO phase, the Mediterranean mean warming rate accelerated while its spatial increasing tendency changed from the westward to the eastward direction.

References

Barnston AG, Livezey RE (1987) Classification, seasonality and persistence of low-frequency atmospheric circulation patterns. Mon Wea Rev 115:1083–1126

Belkin M (2009) Rapid warming of large marine ecosystems. Progr Oceanogr 81:207–213

Berry DI, Kent EC (2009) A new air–sea interaction gridded dataset from ICOADS with uncertainty estimates. Bull Am Meteorol Soc 90(5):645–656

Bethoux JP, Gentili B (1999) Functioning of the Mediterranean Sea: past and present changes related to freshwater input and climate changes. J Mar Syst 20:33–47

Béthoux JP, Gentili B, Raunet J, Tailliez D (1990) Warming trend in the Western Mediterranean deep water. Nature 347:660–662

Bindoff NL, Willebrand J, Artale V et al (2007) Observations: oceanic climate change and sea level. In: Solomon S, Qin D, Manning M, Chen Z, Marquis M, Averyt KB, Tignor M, Miller HL (eds) Climate change 2007: the physical science basis. Contribution of Working Group I to the Fourth Assessment Report of the Intergovernmental Panel on Climate Change. Cambridge University Press, Cambridge

Christensen JH, Hewitson BA, Busuioc A et al (2007) Regional climate projections. In: Solomon S, Qin D, Manning M, Chen Z, Marquis M, Averyt KB, Tignor M, Miller HL (eds) Climate Change 2007: the physical science basis. Contribution of Working Group I to the Fourth Assessment Report of the Intergovernmental Panel on Climate Change. Cambridge University Press, Cambridge

Criado-Aldeanueva F, Del Río J, García-Lafuente J (2008) Steric and mass-induced Mediterranean sea level trends from 14 years of altimetry data. Glob Planet Chang 60(3–4):563–575

Da Silva AM, Young CC, Levitus S (1994) Atlas of surface marine data, vol. 1: algorithms and procedures. NOAA Atlas NESDIS 8. Nat Oceanic and Atmos Admin, Washington DC, p 83

Emery WJ, Thomson RE (1998) Data and their analysis methods in physical oceanography, 1st and 2nd edns. Pergamon, Amsterdam, p 634

Feudale L, Shukla J (2007) Role of Mediterranean SST in enhancing the European heat wave of summer 2003. Geophys Res Lett 34: L03811. doi:10.1029/2006GL027991

Hurrell JW (1995) Decadal trends in the North Atlantic Oscillation, regional temperatures and precipitation. Science 269:676–679

Hurrell JW, Deser C (2009) North Atlantic climate variability: the role of the North Atlantic Oscillation. J Mar Syst 78:28–41

Hurrell JW, Kushnir Y, Visbeck M, Ottersen G (2003) An overview of the North Atlantic Oscillation. In: Hurrell JW, Kushnir Y, Ottersen G, Visbeck M (Eds), The North Atlantic Oscillation, climatic significance and environmental impact. AGU Geophysical Monograph, vol. 134, pp 1–35

Jones PD et al (1997) Extension to the North Atlantic Oscillation using early instrumental pressure observations from Gibraltar and south-west Iceland. Int J Climatol 17(13):1433–1450

Josey SA (2003) Changes in the heat and freshwater forcing of the eastern Mediterranean and their influence on deep water formation. J Geophys Res 108(C7):3237

Josey SA, Somot S, Tsimplis M (2011) Impacts of atmospheric modes of variability on Mediterranean Sea surface heat exchange. J Geophys Res 116:C02032

Lascaratos A, Roether W, Nittis K, Klein B (1999) Recent changes in deep water formation and spreading in the eastern Mediterranean Sea: a review. Progr Oceanogr 44:5–36

Lascaratos A, Sofianos S, Korres G (2003) Interannual variability of atmospheric parameters over the Mediterranean basin from 1945 to 1994. In: Tracking long-term hydrological change in the Mediterranean Sea. Briand, F (ed), CIESM Workshop Series, vol. 16, pp 21–24

Lionello P, Malanotte-Rizzoli P, Boscolo R, Alpert P, Artale V, Li L, Luterbacher J, May W, Trigo R, Tsimplis M, Ulbrich U, Xoplaki E (2006) The Mediterranean climate: an overview of the main characteristics and issues. In: Lionello P, Malanotte-Rizzoli P, Boscolo R (eds) Mediterranean climate variability. Developments in Earth & Environmental Sciences 4, Elsevier, Amsterdam

Luterbacher J, Dietrich D, Xoplaki E, Grosjean M, Wanner H (2004) European seasonal and annual temperature variability, trends, and extremes since 1500. Science 303:1499–1503

Mariotti A (2010) Recent changes in the Mediterranean water cycle: a pathway toward long-term regional hydroclimatic change? J Climate 23:1513–1525

Mariotti A, Dell'Aquila A (2011) Decadal climate variability in the Mediterranean region: roles of large-scale forcings and regional processes. Clim Dyn. doi:10.1007/s00382-011-1056-7

Mariotti A, Struglia MV, Zeng N, K-Lau M (2002) The hydrological cycle in the Mediterranean region and implications for the water budget of the Mediterranean Sea. J Climate 15:1674–1690

Marullo S, Buongiorno Nardelli B, Guarracino M, Santoleri R (2007) Observing the Mediterranean Sea from space: 21 years of Pathfinder-AVHRR sea surface temperatures (1985 to 2005). Re-analysis and validation. Ocean Sci 3:299–310

Marullo S, Artale V, Santoleri R (2011) The SST multi-decadal variability in the Atlantic–Mediterranean region and its relation to AMO. J Climate (in press)

MEDAR/MEDATLAS group (2002) Mediterranean and Black Sea database of temperature, salinity and biogeochemical parameters climatological atlas. In: IFREMER, Brest, 4 CDROM

Nykjaer L (2009) Mediterranean Sea surface warming 1985–2006. Clim Res 39:11–17

Quadrelli R, Pavan V, Molteni F (2001) Wintertime variability of Mediterranean precipitation and its links with large-scale circulation anomalies. Clim Dyn 17:457–466

Rixen M et al (2005) The Western Mediterranean deep water: a proxy for climate change. Geophys Res Lett 32:L12608. doi:10.1029/2005GL022702

Roether W, Manca BB, Klein B, Bregant B, Georgopoulos D, Beitzel V, Kovacevic V, Luchetta A (1996) Recent changes in Eastern Mediterranean deep waters. Science 271:333–335

Romanou A, Tselioudis G, Zerefos CS, Clayson C, Curry JA, Andersson A (2010) Evaporation-precipitation variability over the Mediterranean and the Black Seas from satellite and reanalysis estimates. J Clim 23:5268–5287

Rowell DP (2003) The impact of Mediterranean SSTs on the Sahelian rainfall season. J Climate 16:849–862

Schlesinger ME (1994) An oscillation in the global climate system of period 65–70 years. Nature 367(6465):723–726

Skliris N, Sofianos S, Lascaratos A (2007) Hydrological changes in the Mediterranean Sea in relation to changes in the freshwater budget: a numerical modelling study. J Mar Syst 65:400–416

Skliris N, Mantziafou A, Sofianos S, Ganasos T (2010) Satellite-derived variability of the Aegean Sea ecohydrodynamics. Cont Shelf Res 30:403–418

Somot S, Sevault F, Déqué M, Crépon M (2008) 21st century climate change scenario for the Mediterranean using a coupled atmosphere–ocean regional climate model. Glob Planet Chang 63:112–126

Trigo RM, Osborn TJ, Corte-Real JM (2002) The North Atlantic Oscillation influence on Europe: climate impacts and associated physical mechanisms. Clim Res 20:9–17

Tsimplis MN, Josey SA (2001) Forcing of the Mediterranean Sea by atmospheric oscillations over the North Atlantic. Geophys Res Lett 28:803–806

Vargas-Yáñez M, Moya F, García-Martínez MC, Tel E, Zunino P, Plaza F, Salat J, López-Jurado JL, Serra M (2010) Climate change in the Western Mediterranean Sea 1900–2008. J Mar Syst 82:171–176

Venegas RM, Strub PT, Beier E, Letelier R, Thomas CA, Cowles T, James C, Sotto-Mardones L, Cabrera C (2008) Satellite-derived variability in chlorophyll, wind stress, sea surface height, and temperature in the northern California Current System. J Geophys Res 113:C03015

Xoplaki E, Luterbacher J, Gonzalez-Rouco JF (2006) Mediterranean summer temperature and winter precipitation, large-scale dynamics, trends. IL NUOVO CIMENTO 29:45–54

Yoder JA, Schollaert SE, O'Reilly JE (2002) Climatological phytoplankton chlorophyll and sea surface temperature patterns in continental shelf and slope waters off the northeast U.S. coast. Limnol Oceanogr 47:672–682